Journal of Quantitative Spectroscopy & Radiative Transfer 221 (2018) 129–137

Contents lists available at ScienceDirect

Journal of Quantitative Spectroscopy & Radiative Transfer

journal homepage: www.elsevier.com/locate/jqsrt

High–resolution FTIR spectroscopic study of $^{73}GeH_4$ up to 2300 cm^{-1}

O.N. Ulenikov[a,*], O.V. Gromova[a], E.S. Bekhtereva[a], N.I. Raspopova[a], M.A. Koshelev[b], I.A. Velmuzhova[c], A.D. Bulanov[c], P.G. Sennikov[c]

[a] Research School of High–Energy Physics, National Research Tomsk Polytechnic University, Tomsk 634050, Russia
[b] Institute of Applied Physics, Russian Academy of Sciences, Nizhny Novgorod 603950, Russia
[c] G.G. Devyatykh Institute of Chemistry of High Purity Substances, Russian Academy of Sciences, Nizhny Novgorod 603950, Russia

ARTICLE INFO

Article history:
Received 24 August 2018
Revised 22 September 2018
Accepted 23 September 2018
Available online 26 September 2018

ABSTRACT

The spectra of germane enriched up to 99.9 % of $^{73}GeH_4$ were recorded with a high resolution (0.003 cm^{-1}) at different pressures with the Bruker IFS 125HR Fourier transform spectrometer (Nizhny Novgorod, Russia) in the region of 650–4400 cm^{-1} and analyzed in the Dyad and Pentad region. The 9208 transitions belonging to the seven "cold" bands (6987 transitions) of the Dyad and Pentad and to the nine "hot" Dyad–Pentad bands (2221 transitions) were assigned and theoretically analysed in the frame of the effective Hamiltonian model. The obtained set of 68 fitted parameters reproduces the initial 9208 experimental line positions with the $d_{rms} = 2.82 \times 10^{-4}$ cm^{-1} .

© 2018 Elsevier Ltd. All rights reserved.

1. Introduction

The interest in high resolution study of germane infrared spectra is motivated by several reasons. Firstly, high resolution spectra of germane can be interesting for studying the atmospheres of giant gas-planets, such as Jupiter and Saturn (see, e.g., [1–8]), and its presence should be taken into account when studying their atmospheric composition and chemistry. Germane is used for production of high-purity single–crystal germanium which can be used simultaneously as a source of a double beta decay of its nuclei and as a detector of such processes (see, e.g., Ref [9,10]. For all of these reasons, laboratory investigations of high resolution spectra of germane are timely and important.

Germane $^{M}GeH_4$ in a natural isotopic composition produces complex infrared spectra because of the existence of five stable isotopologues with mass numbers $M = 70$ (20.55%), $M = 72$ (27.37%), $M = 73$ (7.67%), $M = 74$ (36.74%) and $M = 76$ (7.67%) . For that reason, laboratory spectroscopic studies of different germane isotopically enriched samples are preferable. Spectra of different isotopologues of germane have been the objects of study over many years. Up to 1972 spectra were recorded at low or medium resolution. High resolution spectra of germane started being reported on 1973 (see, Refs. [11–33]). In this paper we present the results of the joint high–resolution study of all ro–vibrational bands of $^{73}GeH_4$ (isotopically enriched up to 99.9 %) in the region 650–2300 cm^{-1} where the Dyad and Pentad are located (numerous "hot" Dyad–Pentad transitions belonging to the nine different "hot" bands are also taken into account). The details of our experiment are given in Section 2. In Section 3, the brief theoretical background of our study is presented. Description of the spectra, assignments of transitions and the further theoretical analysis of the experimental data are discussed in Sections 4 and 5.

2. Experimental details

A sample of germane containing 99.9% of the $^{73}GeH_4$ isotopologue was used in the present study. A method of the sample preparation is similar to that described in our previous studies for the $^{76}GeH_4$ isotopologue, Refs [34–36]. Briefly, the sample of germane in natural abundance was synthesized at the Institute of Chemistry of High–Purity Substances of the Russian Academy of Sciences by a reaction between $GeCl_4$ and sodium borohydride with subsequent purification by the rectification method. Then the sample was enriched with the ^{73}Ge isotope using the centrifugal method at the Joint Stock Company Production Association Electrochemical Plant, Zelenogorsk, Russia. The enriched sample was repeatedly purified by the rectification method.

Spectra of the gas sample of germane were recorded using a Bruker IFS125HR Fourier transform spectrometer. The experimental details are presented in Table 1. Briefly, the spectrometer was equipped with a Globar source, a KBr beam splitter and liquid nitrogen cooled mercury–cadmium telluride (MCT) and indium antimonide (InSb) detectors. The sample spectra were recorded with a resolution of 0.003 cm^{-1} (the resolution due to the maximum op-

* Corresponding author.
E-mail address: ulenikov@mail.ru (O.N. Ulenikov).

https://doi.org/10.1016/j.jqsrt.2018.09.023
0022-4073/© 2018 Elsevier Ltd. All rights reserved.

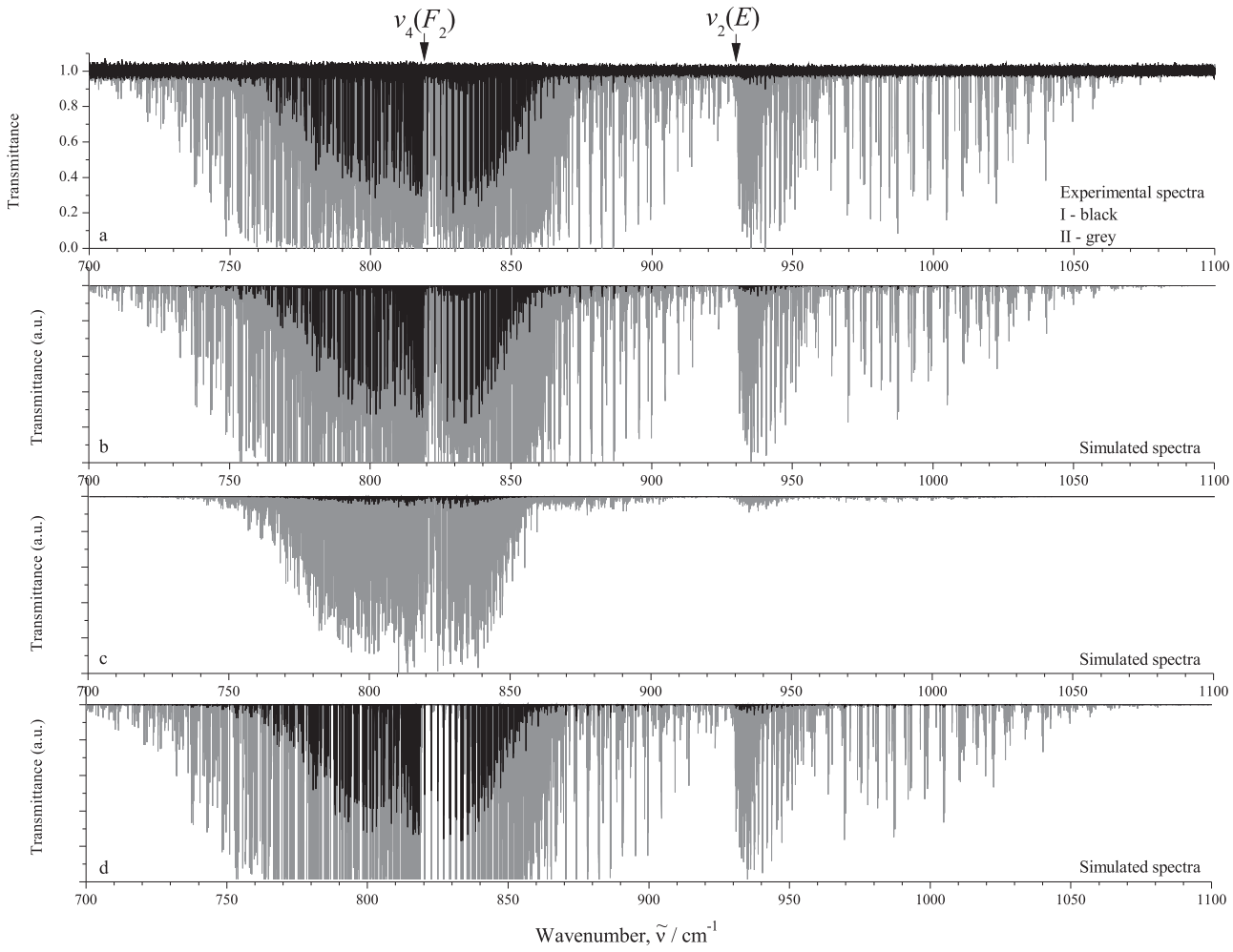

Fig. 1. Survey spectra I and II of $^{73}GeH_4$ (upper trace) in the region of 700–1100 cm^{-1} (for the experimental conditions, see Table 1). Traces 1b–1d present simulated spectra: trace 1d is the simulated spectrum of the ν_2/ν_4 bands; trace 1c is the simulated spectrum of the "hot" Dyad–Pentad bands $2\nu_4(A_1)-\nu_4$, $2\nu_4(E)-\nu_4$, $2\nu_4(F_2)-\nu_4$, $\nu_2+\nu_4(F_2)-\nu_2$, $\nu_2+\nu_4(F_1)-\nu_2$, $\nu_2+\nu_4(F_2)-\nu_4$, $\nu_2+\nu_4(F_1)-\nu_4$, and $2\nu_2(A_1)-\nu_2$; and trace 1b is the sum of separate traces 1c and 1d.

Table 1
Experimental setup for the regions 650–4400 cm^{-1} of the infrared spectra of $^{73}GeH_4$.

Spectrum	Resolution /cm^{-1}	Measuring time/h	No. of scans	Spectral range /cm^{-1}	Detector	Beam-splitter	Opt. path-length/m	Aperture /mm	Temp. /°C	Pressure /Torr
I	0.003	30.2	900	650–2300	MCT	KBr	0.2	1.5	22.0	0.04
II	0.003	36.9	1100	650–2300	MCT	KBr	0.2	1.7	20.8	4.0
III	0.003	33.5	1000	1900–4400	InSb	KBr	3.75	1.0	24.9	0.4
IV	0.003	33.5	1000	1900–4400	InSb	KBr	3.75	1.0	25.3	3.0

tical path difference) in the frequency range 650–2300 cm^{-1} . The Norton–Beer (weak) apodization function was applied. To study both strong and weak lines, spectra were recorded at significantly different pressures and optical path lengths. A single–pass 20 cm length cell and a multi–pass White cell were used. A cell was permanently connected to a gas sample vacuum system, a turbo–molecular pump, and capacitance pressure gauges covering the $10^{-3}-100$ Torr range. The optical compartment of the spectrometer was pumped out by a mechanical pump down to 0.02 Torr (or less) and that pressure remained constant during the experiments.

The final spectra (see Figs. 1 and 3) were obtained by averaging about 1000 scans. In total, four spectra were recorded at two values of optical path length and different pressures. Spectra were calibrated using the most intense and well resolved H_2O and CO_2 lines from the HITRAN database line list, [37]. After calibration the standard deviation of the difference between the measured and tabulated peak positions was estimated to be less than 3×10^{-4} cm^{-1} .

3. Brief theoretical background

Germane is a spherical top molecule of the T_d symmetry. This molecule has a tetrahedral structure resulting in one nondegenerate (q_1, A_1), one doubly degenerate (q_2, E), and two triply degenerate (q_3, F_2) and (q_4, F_2) vibrational modes. It is well known (see, e.g., Refs [38–40]) that ro–vibrational states of such molecules are divided into groups (polyads) of more or less isolated states which interact with each other inside of the polyad. In the present paper we deal with the so–called Dyad (two vibrational states, (0001, F_2) and (0100, E)) and Pentad (five vibrational states which consist of nine sub–states (0010, F_2), (1000, A_1), (0200, A_1), (0200, E), (0101, F_2), (0101, F_1), (0002, A_1), (0002, E) and (0002, F_2)). Two

states of the dyad are strongly interacting. The pair of states (0010, F_2)/(1000, A_1) and seven states (0200, A_1), (0200, E), (0101, F_2), (0101, F_1), (0002, A_1), (0002, E), (0002, F_2) of the Pentad also interact strongly with each other. The analysis shows that interaction of the first two states with the seven overtone/combination states of the Pentad can be neglected for germane.

The high symmetry of the GeH_4 molecule necessitates using a special mathematical formalism (the theory of Irreducible Tensorial Sets, see, e.g., Refs [41–44]) for description of its spectra. Application of the mentioned formalism to the XY_4 (T_d) molecules has been discussed in the spectroscopic literature many times (see, e.g., Refs [45–49]). For that reason we present only briefly the main points necessary for understanding the procedure of calculations with the effective Hamiltonian of the XY_4 spherical top molecule.

As is known from general vibration-rotation theory [50–52], the Hamiltonian of an arbitrary polyatomic molecule can be reduced to a set of the so–called effective Hamiltonians, or, in a more general case, to a set of effective operator matrices of the form (it was discussed in the literature many times, see, e.g., [53,54])

$$H^{vib.-rot.} = \sum_{a,b} |a\rangle\langle b| H^{a,b}, \tag{1}$$

where $|a\rangle$ and $\langle b|$ are the basic vibrational functions; the operators $H^{a,\,b}$ depend on the rotational operators J_α only, and summation is performed in all degenerate and/or interacting vibrational states. When, as in our case, a molecule possesses a symmetry, Eq. (1) can be rewritten in the symmetrized form [45–49]:

$$H^{vib.-rot.} = \sum_{\nu\gamma,\nu'\gamma'} \sum_{n\Gamma} [(|\nu\gamma\rangle \otimes \langle\nu'\gamma'|)^{n\Gamma} \otimes H^{n\Gamma}_{\nu\gamma,\nu'\gamma'}]^{A_1}$$
$$\equiv \sum_{\nu\gamma,\nu'\gamma'} \sum_{n\Gamma} \sum_{\Omega K} [(|\nu\gamma\rangle \otimes \langle\nu'\gamma'|)^{n\Gamma} \otimes R^{\Omega(K,n\Gamma)}]^{A_1} Y^{\Omega(K,n\Gamma)}_{\nu\gamma,\nu'\gamma'}. \tag{2}$$

In Eq. (2): (a). $|\nu\gamma\rangle$ are the symmetrized vibrational functions, γ are symmetries of these functions; $R^{\Omega(K,n\Gamma)}_\sigma$ are symmetrized rotational operators, and Ω is the total degree of the rotational operators J_α ($\alpha = x, y, z$) in the individual operator R; K is the rank of this operator (see, e.g., [55]), Γ is its symmetry in the T_d point symmetry group, and n distinguishes between possible different operators $R^{\Omega(K,n\Gamma)}_\sigma$ having the same values of Ω, K and Γ. The sign $\otimes$ denotes a tensorial product, and the values $Y^{\Omega(K,n\Gamma)}_{\nu\gamma,\nu'\gamma'}$ are different–type spectroscopic parameters.

(b). The symmetrized rotational operators, $R^{\Omega(K,n\Gamma)}_\sigma$, are determined as, [55]),

$$R^{\Omega(K,n\Gamma)}_\sigma = \sum_m {}^{(K)}C^m_{n\Gamma\sigma} R^{\Omega(K)}_m, \tag{3}$$

where the operators $R^{\Omega(K)}_m$ are symmetrized in the SO(3) symmetry group rotational operator which can be constructed in accordance with the recurrence relation, [49,55]:

$$R^{\Omega+1(K+1)}_{\tilde m} = \sum_{l=-1,0,1} C^{K+1\ \tilde m}_{K\ \tilde m-l,1\ l} R^{\Omega(K)}_{\tilde m-l} R^{1(1)}_l, \tag{4}$$

where $C^{K+1\ \tilde m}_{K\ \tilde m-l,1\ l}$ are known Clebsh–Gordan coefficients, Ref [43]. The irreducible rotational operators $R^{\Omega(K)}_m$ with $K < \Omega$ (in this case, the parity of both Ω, and K must be the same, [55]) are constructed as,

$$R^{\Omega(K)}_m = R^{\Omega=K(K)}_m (R^{2(0)})^{(\Omega-K)/2}, \tag{5}$$

where the notation $R^{2(0)} = (J^2_x + J^2_y + J^2_z)$ is used. In this case, the first order and rank operators, $R^{1(1)}_m$ ($m = 0, \pm1$) are determined as

$$R^{1(1)}_1 = -\frac{1}{\sqrt{2}}(J_x - iJ_y) \equiv -J_+,$$
$$R^{1(1)}_{-1} = \frac{1}{\sqrt{2}}(J_x + iJ_y) \equiv J_-,$$
$$R^{1(1)}_0 = J_z \equiv J_0, \tag{6}$$

where

$$J_x = i\frac{\cos\varphi}{\sin\theta}\left(\frac{\partial}{\partial\psi} - \cos\theta\frac{\partial}{\partial\varphi}\right) - i\sin\varphi\frac{\partial}{\partial\theta},$$
$$J_y = -i\frac{\sin\varphi}{\sin\theta}\left(\frac{\partial}{\partial\psi} - \cos\theta\frac{\partial}{\partial\varphi}\right) - i\cos\varphi\frac{\partial}{\partial\theta}, \tag{7}$$

and

$$J_z = -i\frac{\partial}{\partial\varphi}. \tag{8}$$

The values ${}^{(K)}C^m_{n\Gamma\sigma}$ in Eq. (3) are so–called reduction matrix elements, which can be found in the literature (see, e.g., [46], [56], [57]).

4. Description of the spectra and assignment of transitions

The upper parts of Figs. 1 and 3 presents the survey spectra I (black) and II (grey) in the regions of 700–1100 and 1600–2300 cm^{-1} where the bands of the Dyad and Pentad are located. One can see the clearly pronounced strong ν_4 (Fig. 1) and ν_3/ν_1 (Fig. 3) bands and considerably weaker ν_2 (Fig.1) and $2\nu_2/\nu_2 + \nu_4/2\nu_4$ (Fig. 3) bands. Numerous strong lines in Fig. 3 belong to H_2O. Some small fragments of the recorded high resolution spectra are shown at the upper parts of Figs. 2, 4a, 4d and 5.

As was mentioned above, the GeH_4 molecule is a spherical top with a symmetry isomorphic to the T_d point symmetry group. As a consequence, transitions in absorption are allowed only between vibrational states ($v\Gamma$) and ($v'\Gamma'$) for which the relation (see, *e.g.*, [58,59])

$$\Gamma \otimes \Gamma' \in F_2 \tag{9}$$

is fulfilled. Transitions between the vibrational states which do not satisfy the conditions, Eq. (1), are forbidden by the symmetry of a molecule and can appear in the absorption spectra only because of resonance interactions with the allowed ones.

At the first step of the analysis, which was made with the use of results from [60,61], assignments of transitions with $J^{max.} = 8$ was fulfilled for the "cold" bands. We were able to assigned without doubt transitions in the seven bands: $\nu_2(E)$, $\nu_4(F_2)$, $\nu_1(A_1)$, $\nu_3(F_2)$, $\nu_2 + \nu_4(F_2)$, $\nu_2 + \nu_4(F_1)$, and $2\nu_2(E)$. The correctness of these assignments was confirmed by the use of numerous ground state combination differences.

The second analysis step consisted of assignments of ro–vibrational transitions with higher values of the quantum number J of all "cold" bands. In this case, the assignment was made simultaneously with the fit of spectroscopic parameters. Unfortunately, we were not able to assign transitions to the $2\nu_2(A_1)$ and $2\nu_4$ bands. As to the seven other "cold" bands, in general, the 6987 transitions with the quantum number $J^{max.} = 33$ were assigned (see, for details, statistical information in Table 2). That is considerably larger than the number of assigned transitions of the corresponding "cold" bands of the $^{76}GeH_4$ isotopologue in Refs [34–36]. (see Table 2). We would like to mention that 458 transitions of $^{73}GeH_4$ up to $J^{max.} = 23$ were assigned to the $\nu_3(F_2)$ and $\nu_1(A_1)$ bands in the recent study of Boudon, et al.[33]. We have been able to extend their work by assigning 3761 transitions up to $J^{max.} = 33$ in the present study. The list of assigned experimental transitions is presented in the Supplementary materials I, II, and III to this article.

In the third and final step of analysis of the experimental spectra, transitions were assigned which belong to the eight "hot" Dyad–Pentad bands: $2\nu_4(A_1) - \nu_4$, $2\nu_4(E) - \nu_4$, $2\nu_4(F_2) - \nu_4$, $\nu_2 + \nu_4(F_2) - \nu_2$, $\nu_2 + \nu_4(F_1) - \nu_2$, $\nu_2 + \nu_4(F_2) - \nu_4$, $\nu_2 + \nu_4(F_1) - \nu_4$, and $2\nu_2(A_1) - \nu_2$. In general, 2221 transitions were assigned,

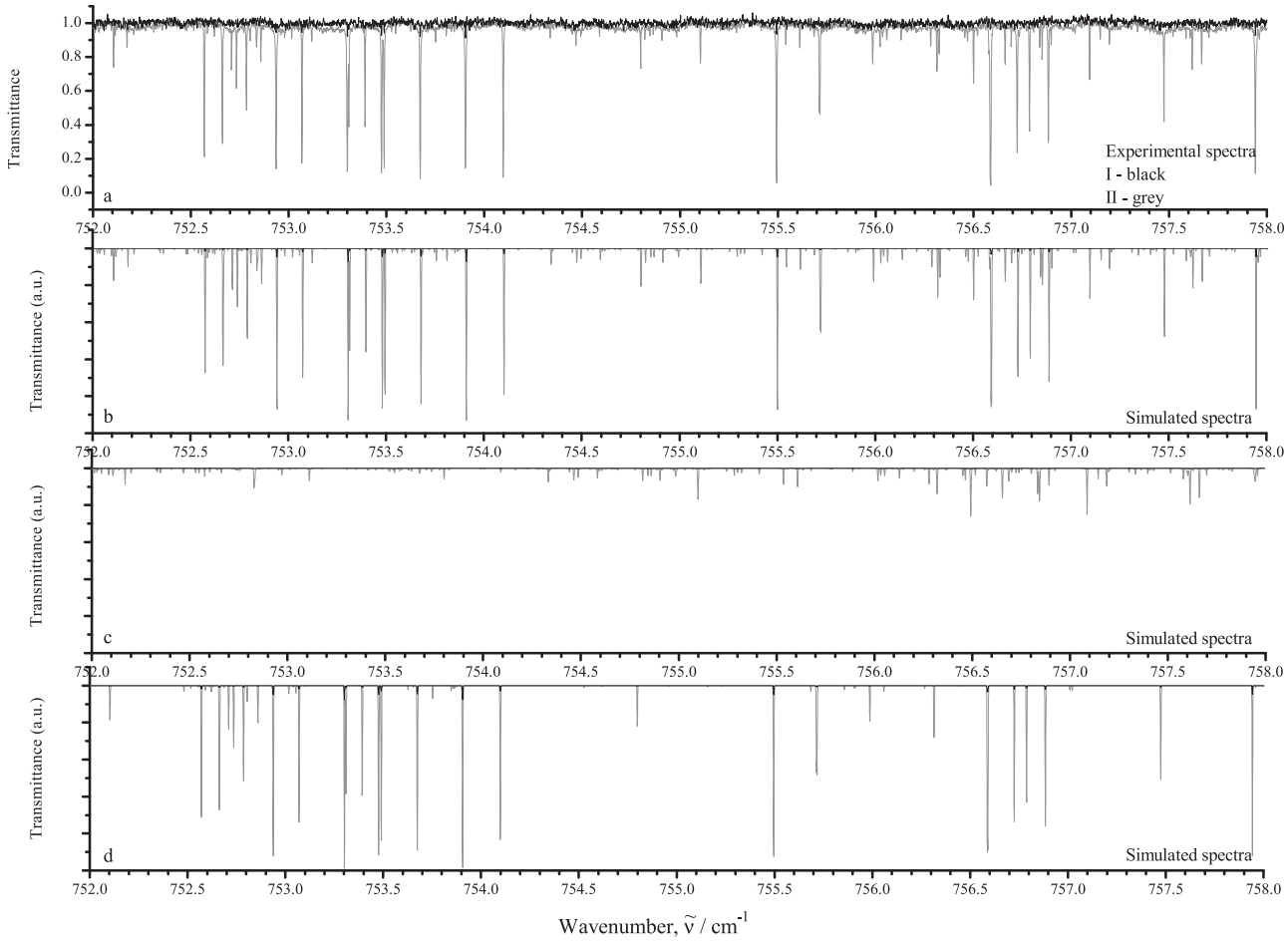

Fig. 2. Fragment of the high resolution spectrum II (trace 2a) of $^{73}GeH_4$ in the P–branch region of the ν_4 band (for the experimental conditions, see Table 1). Traces 2b–2d present simulated spectra: trace 2d is the simulated spectrum of the ν_4 band; trace 2c is the simulated spectrum of the "hot" Dyad–Pentad bands; trace 2b is the sum of separate traces 2c and 2d.

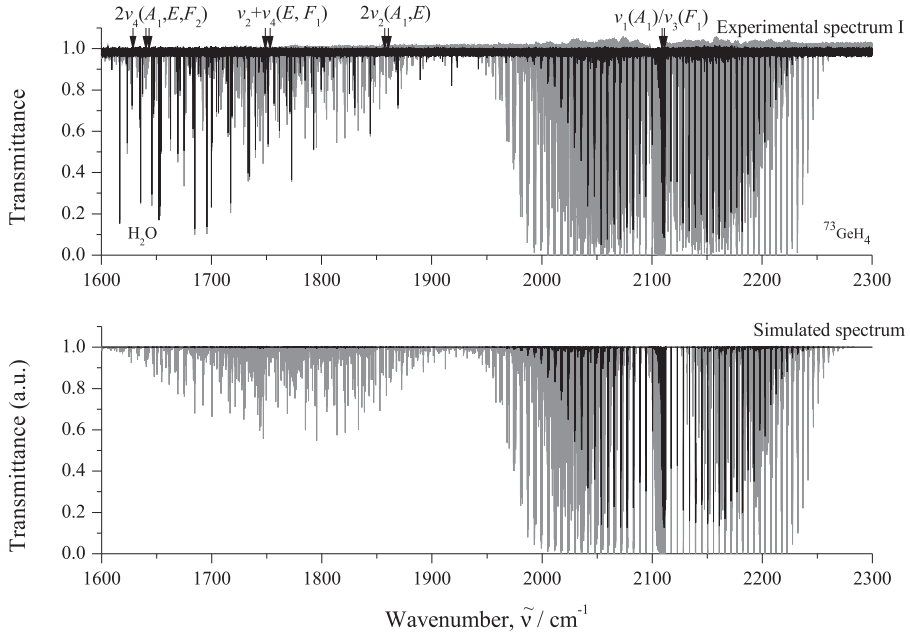

Fig. 3. Survey spectra I and II of $^{73}GeH_4$ (upper trace) in the region of 1600–2300 cm^{-1} (for the experimental conditions, see Table 1). The corresponding simulated spectra are presented on the lower part of Fig. 3.

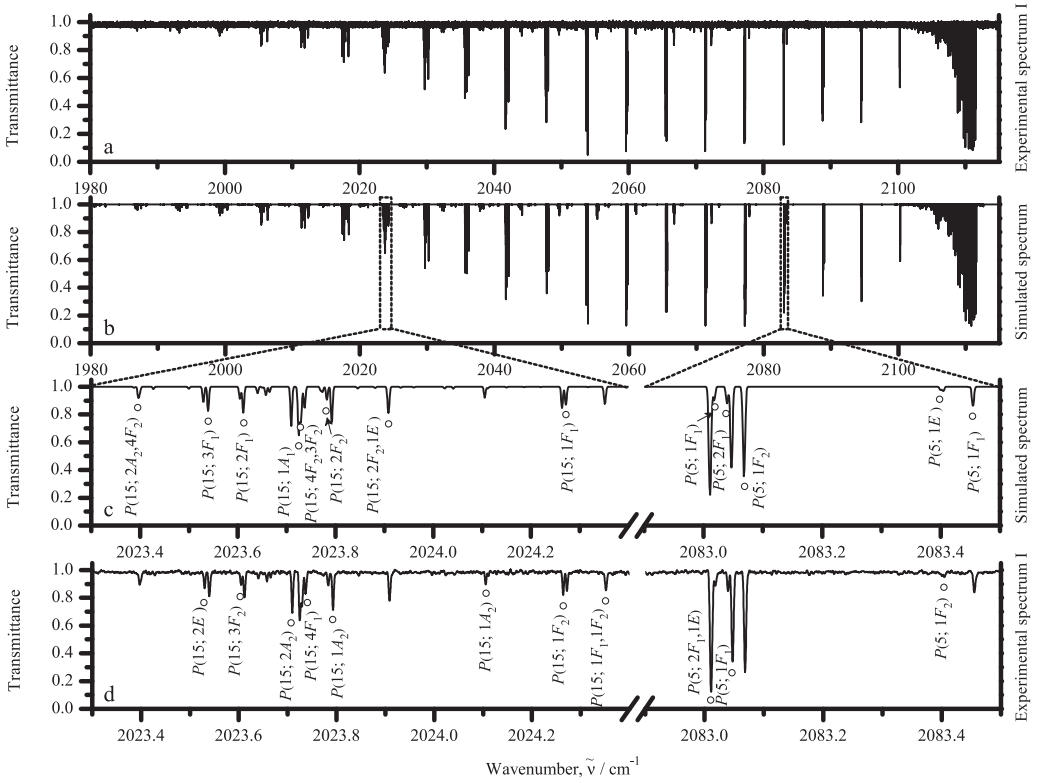

Fig. 4. Small parts (Figs. 4 a and d) of the high resolution spectrum I of $^{73}GeH_4$ in the P–branch region of the ν_3/ν_1 bands with examples of transitions assigned to the ν_3 band. (for the experimental conditions see Table 1). Figs. 4 b and c present the corresponding simulated spectrum of $^{73}GeH_4$ in this region (see text for details).

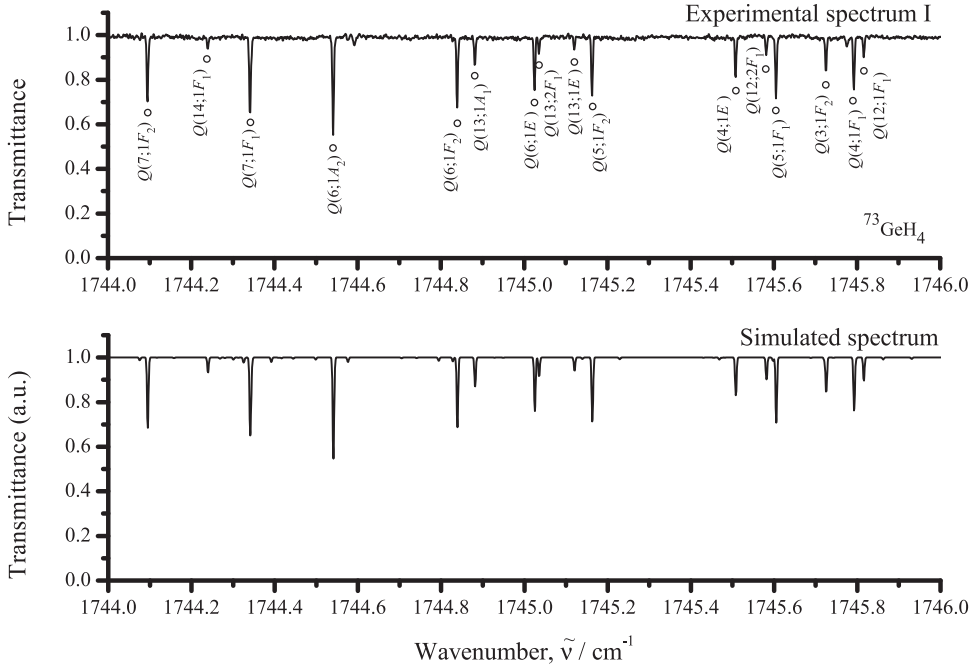

Fig. 5. Small part of the high resolution spectrum II (upper part) of $^{73}GeH_4$ in the Q–branch region of the $\nu_2 + \nu_4(F_2)$ band with examples of transitions assigned to this band (for the experimental conditions see Table 1). The lower part of the figure presents the corresponding simulated spectrum.

that is about 2.3 times larger than in the corresponding spectra of $^{76}GeH_4$ in Ref [36]. A complete list of the "hot" assigned experimental transitions is added to the Supplementary material I (see also statistical information in Table 2). Adding the "hot" transitions to the "cold" ones has allowed us to obtain upper state ro–vibrational energy levels for all vibrational states of the Dyad and Pentad. In summary, 3832 ro–vibrational energy values from all eleven upper vibrational states, (0001, F_2) and (0100, E) of the Dyad and (0010, F_2), (1000, A_1), (0200, A_1), (0200, E), (0101, F_2),

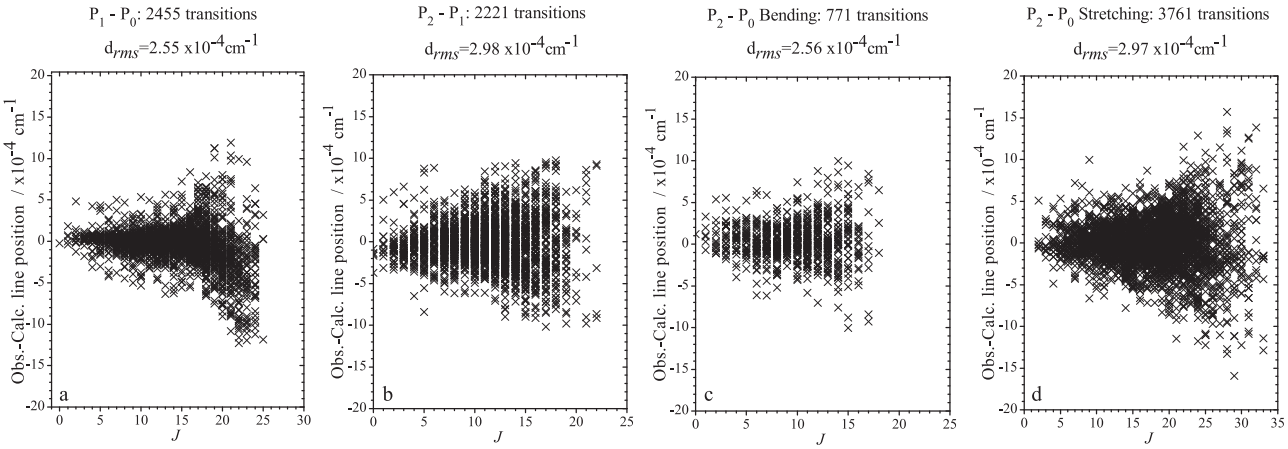

Fig. 6. Observed – calculated line positions and fit statistics for bands studied in the present paper: Figs. 6a–6d correspond to the bands of the Dyad, to the "hot" bands of the Dyad–Pentad, to a set of the bending bands of the Pentad, and to the two stretching bands of the Pentad, respectively.

Table 2
Statistical information for the Dyad and Pentad of $^{73}GeH_4$.

Band 1	Center/cm^{-1} 2	J^{max} 3	N_{tr}[a] 4	m_1[b] 5	m_2[b] 6	m_3[b] 7
ν_4, F_2 $^{73}GeH_4$ tw[c]	820.91109	25	1296	78.9	11.5	9.6
ν_4, F_2 $^{76}GeH_4$ [34]	820.32700	26	1117			
ν_2, E $^{73}GeH_4$ tw[c]	929.90700	24	1159	78.2	13.2	8.6
ν_2, E $^{76}GeH_4$ [34]	929.91303	23	805			
ν_3, F_2 $^{73}GeH_4$ tw[c]	2111.35458	33	2714	66.2	20.6	13.2
ν_3, F_2 $^{73}GeH_4$ [34]	2111.35474	23	458			
ν_3, F_2 $^{76}GeH_4$ [35]	2110.73231	31	1366	77.5	19.2	3.3
ν_1, A_1 $^{73}GeH_4$ tw[c]	2110.70427	28	1047	74.7	17.9	7.4
ν_1, A_1 $^{76}GeH_4$ [35]	2110.69177	20	445	78.5	16.9	5.6
$\nu_2+\nu_4$, F_2 $^{73}GeH_4$ tw[c]	1748.97477	18	465	72.1	18.9	9.0
$\nu_2+\nu_4$, F_2 $^{76}GeH_4$ [36]	1748.3962	19	793	61.1	27.4	11.5
$\nu_2+\nu_4$, F_1 $^{73}GeH_4$ tw[c]	1753.08488	16	294	70.8	24.1	5.1
$\nu_2+\nu_4$, F_1 $^{76}GeH_4$ [36]	1752.5031	18	699	65.3	24.4	10.3
$2\nu_2$, E $^{73}GeH_4$ tw[c)]	1860.65568	14	12	41.7	50.1	8.2
$2\nu_2$, E $^{76}GeH_4$ [36]	1860.6673	19	503	78.4	13.9	7.7
$2\nu_4$, $A_1-\nu_4$ $^{73}GeH_4$ tw[c]	807.73698	19	268	66.3	18.2	15.5
$2\nu_4$, $A_1-\nu_4$ $^{76}GeH_4$ [36]		11	76	76.3	17.1	6.6
$2\nu_4$, $E-\nu_4$ $^{73}GeH_4$ tw[c]	822.39494	19	171	70.8	15.8	13.4
$2\nu_4$, $E-\nu_4$ $^{76}GeH_4$ [36]		15	52			
$2\nu_4$, $F_2-\nu_4$ $^{73}GeH_4$ tw[c]	819.50097	22	665	60.8	22.7	16.5
$2\nu_4$, $F_2-\nu_4$ $^{76}GeH_4$ [36]		15	206			
$\nu_2+\nu_4$, $F_2-\nu_2$ $^{73}GeH_4$ tw[c]	819.06777	19	399	64.5	25.1	10.4
$\nu_2+\nu_4$, $F_2-\nu_2$ $^{76}GeH_4$ [36]		15	236			
$\nu_2+\nu_4$, $F_1-\nu_2$ $^{73}GeH_4$ tw[c]	823.17788	19	394	68.6	21.0	10.4
$\nu_2+\nu_4$, $F_1-\nu_2$ $^{76}GeH_4$ [36]		15	179			
$\nu_2+\nu_4$, $F_2-\nu_4$ $^{73}GeH_4$ tw[c]	928.06368	16	133	62.0	27.3	10.7
$\nu_2+\nu_4$, $F_2-\nu_4$ $^{76}GeH_4$ [36]		16	119			
$\nu_2+\nu_4$, $F_1-\nu_4$ $^{73}GeH_4$ tw[c]	932.17379	17	69	58.0	33.3	8.7
$\nu_2+\nu_4$, $F_1-\nu_4$ $^{76}GeH_4$ [36]		15	45			
$2\nu_2$, $A_1-\nu_2$ $^{73}GeH_4S$ tw[c]	1857.260697	14	8	50.0	37.5	12.5
$2\nu_2$, $E-\nu_2$ $^{73}GeH_4$ tw[c]	1857.260697	19	114	76.3	18.4	5.3
$2\nu_2$, $E-\nu_2$ $^{73}GeH_4$ tw [36]		17	81			

[a] N_{tr} is the number of assigned transitions.
[b] Here $m_i = n_i/N_{tr} \times 100\%$ (i = 1, 2, 3); n_1, n_2, and n_3 are the numbers of transitions for which the differences $\delta = \nu^{exp} - \nu^{calc}$ satisfy the conditions $\delta \le 2 \times 10^{-4}$ cm^{-1}, 2×10^{-4} cm^{-1} $< \delta \le 4 \times 10^{-4}$ cm^{-1}, and $\delta > 4 \times 10^{-4}$ cm^{-1}, respectively.
[c] The "tw" means "this work".

(0101, F_1), (0002, A_1), (0002, E) and (0002, F_2) of the Dyad and Pentad were obtained.

5. Parameters of the effective Hamiltonian

All the 9208 experimental transitions discussed in the before section were used as the initial information in the weighted fit procedure of determination of the effective Hamiltonian, Eq. (2), parameters. The results of the fit are presented in column 4 of Table 3 together with their 1σ confidence statistical intervals (the latter are given in parentheses). Parameters in Table 3, which are shown without parentheses, have been constrained to the corresponding values of parameters of the $^{76}GeH_4$ species from Refs [34–36]. Correctness of the obtained results is confirm by the fact that 68 parameters, obtained from the fit in the present study, reproduce the 9208 initial experimental line positions with the $d_{rms} = 2.82 \times 10^{-4}$ cm^{-1}. Columns 5 of the Supplementary materials present the values of differences $\delta = (\nu^{exp.} - \nu^{calc.})$ in units of 10^{-4} cm^{-1} between the experimental line positions and ones calculated with the parameters from Table 3; and Fig. 6 shows the fit

Table 3
Spectroscopic parameters $Y^{\Omega(K,n\Gamma)}_{v\gamma,v'\gamma'}$ of the Dyad and Pentad of $^{73}GeH_4$ (in cm^{-1})[a].

(v, γ) 1	(v', γ') 2	$\Omega(K, n\Gamma)$ 3	$^{73}GeH_4$ 4	(v, γ) 1	(v', γ') 2	$\Omega(K, n\Gamma)$ 3	$^{73}GeH_4$ 4
(0000, A_1)	(0000, A_1)	2(0, A_1)	2.69586298(11)		(0101, F_2)	3(1, F_1)10^4	-0.18456
	(0000, A_1)	4(0, A_1)10^4	-0.3341682		(0101, F_2)	3(3, F_1)10^4	-0.14931
	(0000, A_1)	4(4, A_1)10^5	-0.1547079	(0101, F_1)	(0002, A_1)	1(1, F_1)	0.0654326(76)
	(0000, A_1)	6(0, A_1)10^8	0.114368	(0101, F_1)	(0002, E)	1(1, F_1)10^3	0.2899(58)
	(0000, A_1)	6(4, A_1)10^{10}	-0.51075	(0101, F_1)	(0002, F_2)	1(1, F_1)10^2	-0.11623(61)
	(0000, A_1)	6(6, A_1)10^{10}	-0.15638		(0002, F_2)	2(2, E)10^3	0.15405(14)
(0100, E)	(0100, E)	0(0, A_1)	929.9070022(47)		(0002, F_2)	2(2, F_2)10^5	0.1592(11)
	(0100, E)	2(2, E)10^1	-0.10788781		(0002, F_2)	3(1, F_2)10^5	-0.2948(15)
	(0100, E)	3(3, A_2)10^4	0.22618		(0002, F_2)	3(3, A_2)10^5	0.3359
	(0100, E)	4(0, A_1)10^6	-0.4052		(0002, F_2)	3(3, F_1)10^5	-0.9951
	(0100, E)	4(2, E)10^6	-0.31077		(0002, F_2)	3(3, F_2)10^6	0.692(13)
	(0100, E)	4(4, A_1)10^7	0.134	(0101, F_2)	(0002, A_1)	2(2, F_2)10^3	0.3879
	(0100, E)	4(4, E)10^6	-0.12583		(0002, A_1)	3(3, F_2)10^5	-0.2096(17)
(0100, E)	(0001, F_2)	1(1, F_1)	-4.507623(21)	(0101, F_2)	(0002, E)	3(1, F_1)10^4	-0.14428(13)
	(0001, F_2)	2(2, F_2)	-0.02129422(14)	(0101, F_2)	(0002, F_2)	0(0, A_1)	-4.301686(78)
	(0001, F_2)	3(1, F_1)10^3	-0.1179267		(0002, F_2)	1(1, F_1)	0.0257799(46)
	(0001, F_2)	3(3, F_2)10^4	0.138096		(0002, F_2)	2(0, A_1)10^3	0.63352
	(0001, F_2)	4(2, F_2)10^6	-0.2122		(0002, F_2)	2(2, E)10^4	-0.2856
	(0001, F_2)	4(4, F_1)10^6	-0.18552		(0002, F_2)	3(1, F_1)10^5	-0.13438(87)
	(0001, F_2)	4(4, F_2)10^6	-0.209879		(0002, F_2)	3(3, F_2)10^4	0.14725
	(0001, F_2)	5(1, F_1)10^8	-0.23013	(0002, A_1)	(0002, A_1)	0(0, A_1)	-13.043719(13)
	(0001, F_2)	5(3, F_1)10^8	0.13677		(0002, A_1)	2(0, A_1)10^4	0.1675(15)
	(0001, F_2)	5(3, F_2)10^9	0.5885	(0002, A_1)	(0002, E)	2(2, E)10^3	0.215498(83)
(0001, F_2)	(0001, F_2)	0(0, A_1)	820.9110861(57)	(0002, A_1)	(0002, F_2)	2(2, F_2)10^3	-0.300740(76)
	(0001, F_2)	1(1, F_1)	6.3819626(18)		(0002, F_2)	3(3, F_2)10^4	0.10079(13)
	(0001, F_2)	2(0, A_1)10^2	0.1070517(47)	(0002, E)	(0002, E)	0(0, A_1)	1.4839987(98)
	(0001, F_2)	2(2, E)10^2	-0.1504833(70)		(0002, E)	2(2, E)10^3	-0.521560(94)
	(0001, F_2)	2(2, F_2)	-0.010695948(64)		(0002, E)	3(3, A_2)10^4	0.10591
	(0001, F_2)	3(1, F_1)10^4	0.704118(53)	(0002, E)	(0002, F_2)	1(1, F_1)	0.0302548(15)
	(0001, F_2)	3(3, F_1)10^4	-0.479437(47)		(0002, F_2)	2(2, F_2)10^3	-0.600092(74)
	(0001, F_2)	4(0, A_1)10^6	-0.3653		(0002, F_2)	3(1, F_1)10^6	-0.3530
	(0001, F_2)	4(2, F_2)10^6	-0.3519		(0002, F_2)	3(3, F_1)10^5	-0.1960
	(0001, F_2)	4(4, A_1)10^7	-0.6407		(0002, F_2)	3(3, F_2)10^5	-0.5111
	(0001, F_2)	5(1, F_1)10^8	0.25953	(0002, F_2)	(0002, F_2)	0(0, A_1)	-1.2393934(83)
	(0001, F_2)	5(3, F_1)10^8	-0.16967		(0002, F_2)	1(1, F_1)	-0.0330830(82)
	(0001, F_2)	6(0, A_1)10^{10}	0.4276		(0002, F_2)	2(0, A_1)10^4	-0.1478
(0200, A_1)	(0200, A_1)	0(0, A_1)	-2.6836900		(0002, F_2)	2(2, E)10^3	0.1190
	(0200, A_1)	2(0, A_1)10^3	-0.4716		(0002, F_2)	2(2, F_2)10^3	0.58844(12)
(0200, A_1)	(0200, E)	2(2, E)10^3	-0.259660(13)		(0002, F_2)	3(1, F_1)10^6	-0.3567(67)
(0200, E)	(0200, E)	0(0, A_1)	0.841533(13)		(0002, F_2)	3(3, F_1)10^5	-0.5775
	(0200, E)	2(2, E)10^3	0.3393	(1000, A_1)	(1000, A_1)	0(0, A_1)	2110.7042698(81)
	(0200, E)	3(3, A_2)10^5	0.26045		(1000, A_1)	2(0, A_1)10^2	-1.7988113(64)
(0200, A_1)	(0101, F_2)	2(2, F_2)10^3	-0.1180		(1000, A_1)	4(0, A_1)10^6	0.17727(11)
(0200, E)	(0101, F_1)	1(1, F_1)	0.0267431(55)		(1000, A_1)	4(4, A_1)10^8	-0.4386(13)
	(0101, F_1)	2(2, F_2)10^3	-0.21017	(1000, A_1)	(0010, F_2)	2(2, F_2)10^2	-0.8095009(36)
	(0101, F_1)	3(3, F_2)10^5	-0.4234		(0010, F_2)	3(3, F_2)10^5	-0.170815(52)
(0200, E)	(0101, F_2)	1(1, F_1)	0.0317455(20)		(0010, F_2)	4(2, F_2)10^6	-0.111586(27)
	(0101, F_2)	3(1, F_1)10^5	-0.4543		(0010, F_2)	4(4, F_2)10^6	-0.158576(39)
(0200, A_1)	(0002, A_1)	0(0, A_1)	-5.45804(21)		(0010, F_2)	5(5, F_2)10^9	0.2873
	(0002, A_1)	2(0, A_1)10^3	0.52441(79)	(0010, F_2)	(0010, F_2)	0(0, A_1)	2111.3545845(41)
(0200, E)	(0002, E)	0(0, A_1)	0.176567(95)		(0010, F_2)	1(1, F_1)	-0.55907227(74)
	(0002, E)	2(2, E)10^3	0.46393(32)		(0010, F_2)	2(0, A_1)	-0.014700452(25)
(0200, E)	(0002, F_2)	1(1, F_1)	0.230860		(0010, F_2)	2(2, E)10^2	0.2263509(33)
	(0002, F_2)	3(1, F_1)10^5	-0.3016		(0010, F_2)	2(2, F_2)10^2	-0.4472682(18)
(0101, F_1)	(0101, F_1)	0(0, A_1)	2.2667942(74)		(0010, F_2)	3(1, F_1)10^5	-0.75253(13)
	(0101, F_1)	1(1, F_1)	-0.0510521		(0010, F_2)	3(3, F_1)10^5	-0.65737(12)
	(0101, F_1)	2(0, A_1)10^5	-0.5090(59)		(0010, F_2)	4(0, A_1)10^8	0.3970(37)
	(0101, F_1)	2(2, F_2)10^3	-0.7694		(0010, F_2)	4(2, E)10^7	0.91672(28)
(0101, F_1)	(0101, F_2)	1(1, F_1)	-0.0564385(23)		(0010, F_2)	4(2, F_2)10^7	-0.6775
	(0101, F_2)	2(2, E)10^4	0.7774		(0010, F_2)	4(4, A_1)10^7	0.10694
	(0101, F_2)	2(2, F_2)10^3	0.79071		(0010, F_2)	4(4, E)10^7	0.1407
	(0101, F_2)	3(1, F_1)10^5	-0.58181		(0010, F_2)	4(4, F_2)10^6	-0.20740
(0101, F_2)	(0101, F_2)	0(0, A_1)	-2.0140333(86)		(0010, F_2)	5(1, F_1)10^9	-0.558
	(0101, F_2)	1(1, F_1)	-0.548272(85)		(0010, F_2)	5(3, F_1)10^9	-0.18787(90)
	(0101, F_2)	2(0, A_1)10^3	-0.37902		(0010, $1F_2$)	5(5, F_1)10^9	0.34126(60)
	(0101, F_2)	2(2, E)10^3	0.3357		(0010, $3F_2$)	5(5, F_1)10^9	-0.66037(99)
	(0101, F_2)	2(2, F_2)10^3	-0.8515				

[a] Values in parentheses are 1σ statistical confidence intervals. Parameters presented without confidence intervals were constrained to the values of corresponding parameters of the $^{76}GeH_4$ isotopologue from Ref. [35].

statistics for the studied bands. Figs. 1b–1d and 2b–2d, lower part of Fig. 3, and Figs. 4b, 4c show the simulated spectra which correspond to the experimental spectra presented in the same figures (one can see a good correspondence between the experimental and simulated spectra). It is necessary to remark that in the procedure of spectral simulation (with the exception of the ν_3/ν_1 bands) we calculated only the relative line strengths. For the ν_3/ν_1 bands, absolute line strengths were calculated with the effective dipole moment parameters from Ref [33]. In all simulations a Doppler line profile was used.

6. Conclusion

In the present study we have recorded high resolution spectra and analyzed these spectra for the $^{73}GeH_4$ molecule in the region of its Dyad and Pentad. The 6987 transitions of the seven "cold" bands and 2221 "hot" bands of $^{73}GeH_4$ were assigned. That is considerably larger in comparison with reported literature data on any isotopologue of germane. On that basis, 3832 ro–vibrational energy values from all eleven upper vibrational states, (0001, F_2) and (0100, E) of the Dyad plus (0010, F_2), (1000, A_1), (0200, A_1), (0200, E), (0101, F_2), (0101, F_1), (0002, A_1), (0002, E) and (0002, F_2) of the Pentad were obtained. The 9208 experimental line positions were used then in the fit of parameters of the effective Hamiltonian, Eq. (1). The obtained set of 68 parameters reproduces the 9208 initial experimental line positions with the $d_{rms} = 2.82 \times 10^{-4}$ cm^{-1}.

Acknowledgments

This research was founded by the Russian Science Foundation, project 18–12–00058.

Supplementary material

Supplementary material associated with this article can be found, in the online version, at 10.1016/j.jqsrt.2018.09.023

References

[1] Fink U, Larson HP, Treffers RR. Germane in the atmosphere of jupiter.. Icarus 1978;34:344–54.
[2] Kunde V, Hanel R, Maguire W, Gautier D, J-P B, Marten A, Chédin A, Husson N, Scott N. The tropospheric gas composition of the north equatorial belt (NH_3, PH_3, CH_3D, GeH_4, H_2O) and the jovian D/H isotopic ratio. Astrophys J 1982;263:443–67.
[3] Drossart P, Encrenaz T, Kunde V, Hanel R, Combes M. An estimate of the PH_3, NH_3, CH_3D and geh_4 abundances on jupiter from the voyager IRIS data at 4.5 µm. Icarus 1982;49:416–26.
[4] Chen F, Judge DL, Wu CYR, Caldwell J, White HP, Wagener R. High--resolution, low–temperature photoabsorption cross sections of C_2-H_2, PH_3, AsH_3, and GeH_4, with application to saturn's atmosphere. J Geophys Res 1991;96:17519–27.
[5] Atreya SK, Mahaffy PR, Niemann HB, Wong MH, Owen TC. Composition and origin of the atmosphere of Jupiter - an update, and implications for the extrasolar giant planets. Planet Space Sci 2003;51:105–12.
[6] Lodders K. Jupiter formed with more tar than ice. Astrophys J 2004;611:587–97.
[7] Asplund M, Grevesse N, Sauval J, Scott P. The chemical composition of the sun. Ann Rev Astron Astrophys 2009;47:451–522.
[8] Lodders K. Atmospheric chemistry of the gas giant planets. Geochemical Society; 2010. http://www.geochemsoc.org/publications/geochemicalnews/gn142jan10/atmosphericchemistryoftheg/
[9] Agostini M, Allardt M, Andreotti E, Bakalyarov AM, Balata M, Barabanov I, et al. The background in the $0\nu\beta\beta$ experiment GERDA. Eur Phys J 2014;74:1–25.
[10] Haller EE. Germanium: from its discovery to sige devices. Mater Sci Semicond Process 2006;9:408–22.
[11] Curl RF, Oka T, Smith DS. The observation of a pure rotational q-branch transition of methane by infrared-radio frequency double resonance. J Mol Spectrosc 1973;46:518–20.
[12] Curl Jr R.F.. Infrared-radio frequency double resonance observations of pure rotational Q-branch transitions of methane *J Mol Spectrosc*. 1973. 48: 165–173.
[13] Kreiner WA, Oka T. Infrared radio-frequency double resonance observations of $\delta j = 0$ "forbidden" rotational transitions of SiH_4. Can J Phys 1975;53:2000–6.
[14] Kreiner WA, Andresen U, Oka T. Infrared-microwave double resonance spectroscopy of GeH_4. J Chem Phys 1977;66:4662–5.
[15] Kreiner WA, Orr BJ, Andresen U, Oka T. Measurement of the centrifugal-distortion dipole moment of GeH_4 using a CO_2 laser. Phys Rev A 1977;15:2298–304.
[16] Kagann RH, Ozier I, Gerry MCL. The centrifugal distortion dipole moment of silane. J Chem Phys 1976;64:3487–8.
[17] Lepage P, Brégier R, Saint-Loup R. La bande ν_3 du germane. c. R Acad Sci Ser-B 1976;B283:179–80.
[18] Kagann RH, Ozier I, McRae GA, Gerry MCL. The distortion moment spectrum of GeH_4: the microwave Q branch. Can J Phys 1979;57:593–600.
[19] Daunt SJ, Halsey GW, Fox K, Lovell RJ, Gailar NM. High-resolution infrared spectra of ν_3 and $2\nu_3$ of germane. J Chem Phys 1978;68:1319–21.
[20] Fox K, Halsey GW, Daunt SJ, Kennedy RC. Transition moment for ν_3 of $^{74}GeH_4$. J Chem Phys 1979;70:5326–7.
[21] Kreiner WA, Magerl G, Furch B, Bonek E. IR laser sideband observations in GeH_4 and CD_4. J Chem Phys 1979;70:5016–20.
[22] Magerl G, Schupita W, Bonek E, Kreiner WA. Observation of the isotope effect in the ν_2 fundamental of germane. J Chem Phys 1980;72:395–8.
[23] Kreiner WA, Opferkuch R, Robiette AG, Turner PH. The ground–state rotational constants of germane. J Mol Spectrosc 1981;85:442–8.
[24] Lepage P, Champion JP, Robiette AG. Analysis of the ν_3 and ν_1 infrared bands of GeH_4. J Mol Spectrosc 1981;89:440–8.
[25] Schaeffer RD, Lovejoy RW. Absolute line strengths of $^{74}GeH_4$ near 5 µm. J Mol Spectrosc 1985;113:310–14.
[26] Zhu Q, Thrush BA, Robiette AG. Local mode rotational structure in the (3000) Ge-H stretching overtone ($3\nu_3$) of germane. Chem Phys Lett 1988;150:181–3.
[27] Zhu Q, Thrush BA. Rotational structure near the local mode limit in the (3000) band of germane. J Chem Phys 1990;92:2691–7.
[28] Zhu Q, Qian H, Thrush BA. Rotational analysis of the (2000) and (3000) bands and vibration-rotation interaction in germane local mode states. Chem Phys Lett 1991;186:436–40.
[29] Campargue A, Vetterhöffer J, Chenevier M. Rotationally resolved overtone transitions of $^{70}GeH_4$ in the visible and near-infrared. Chem Phys Lett 1992;192:353–6.
[30] Zhu Q, Campargue A, Vetterhöffer J, Permogorov D, Stoeckel F. High resolution spectra of GeH_4 v = 6 and 7 stretch overtones. the perturbed local mode vibrational states. J Chem Phys 1993;99:2359–64.
[31] Sun F, Wang X, Liao J, Zhu Q. The (5000) local mode vibrational state of germane: a high-resolution spectroscopic study.. J Mol Spectrosc 1997;184:12–21.
[32] Chen XY, Lin H, Wang XG, Deng K, Zhu QS. High-resolution fourier transform spectrum of the (4000) local mode overtone of GeH_4: local mode effect. J Mol Struct 2000:41–51. 517–518
[33] Boudon V, Grigoryan T, Philipot F, Richard C, Tchana F, Manceron L, Rizopoulos A, Vander Auwera J, Encrenaz T. Line positions and intensities for the ν_3 band of 5 isotopologues of germane for planetary applications. J Quant Spectrosc Radiat Transfer 2018;205:174–83.
[34] Ulenikov ON, Gromova OV, Bekhtereva ES, Raspopova NI, Sennikov PG, Koshelev MA, et al. High resolution study of $^{M}GeH_4 (m = 76, 74)$ in the dyad region. J Quant Spectrosc Radiat Transf 2014;144:11–26.
[35] Koshelev MA, Velmuzhov AP, Velmuzhova IA, Sennikov PG, Raspopova NI, Bekhtereva ES, et al. High resolution study of strongly interacting $\nu_1(a_1)/\nu_3(f_2)$ bands of $^{M}GeH_4 (m = 76, 74)$. J Quant Spectrosc Radiat Transf 2015;164(1):61–74.
[36] Ulenikov ON, Gromova OV, Bekhtereva ES, Raspopova NI, Sennikov PG, Koshelev MA, et al. First high resolution ro–vibrational study of the (0200), (0101) and (0002) vibrational states of $^{M}GeH_4 (m = 76, 74)$. J Quant Spectrosc Radiat Transf 2016;182:199–218.
[37] Gordon IE, Rothman LS, Hill C, Kochanov RV, Tan Y, Bernath PF, et al. The HITRAN 2016 molecular spectroscopic database. J Quant Spectrosc Radiat Transf 2017;203:3?69.
[38] Hecht T. The vibration-rotation energies of tetrahedral XY_4 molecules:Part I theory of spherical top molecules. J Mol Spectrosc 1960;5:355–89.
[39] Niederer HM. Teh Infrared Spectrum of Methane. München: Verlag Dr. Hut; 2012.
[40] Niederer HM, Wang XG, Carrington T, Albert S, Bauerecker S, Boudon V Quack M. Analysis of the rovibrational spectrum of $^{13}CH_4$ in the octad range. J Mol Spectrosc 2013;291:33–47.
[41] Fano U, Racah G. Irreducible Tensorial Sets. New York: Academic Press; 1959.
[42] Wigner EP. Quantum Theory of Angular Momentum. New York: Academic Press; 1965.
[43] Varshalovitch DA, Moskalev AN, Khersonsky VK. Quantum Theory of Angular Momentum. Leningrad: Nauka; 1975.
[44] Boudon V, Champion JP, Gabard T, Loëte M, Wenger RM. Spherical top theory and molecular spectra. In: Quack M, Merkt F, editors. Handbook of High-Resolution Spectroscopy. Wiley; 2011. p. 1437–60. Editors, vol. 3
[45] Moret-Bailly J. Sur l'interprétation des spectres de vibration-rotation des molécules à symmétrie tétraédrique ou octaédrique. Cah Phys 1961;15:238–314.
[46] Champion JP, Pierre G, Michelot F, Moret-Bailly J. Composantes cubiques normales des tenseurs spheriques. Can J Phys 1977;55:512–20.
[47] Champion JP. Developpement complet de l'hamiltonien de Vibration–Rotation adapté à1ı étude des interactions dans les molécules toupies sphériques. application aux bandes ν_2 et ν_4 de $^{12}CH_4$. Can J Phys 1977;55:1802–28.
[48] Boudon V, Champion JP, Gabard T, Loëte M, Michelot F, Pierre G, Rotger M, Wenger C, Rey M. Symmetry–adapted tensorial formalism to model rovibra-

tional and rovibronic spectra of molecules pertaining to various point groups. J Mol Spectrosc 2004;228:620–34.
[49] Cheglokov AE, Ulenikov ON, Zhilyakov AS, Cherepanov VN, YuS M, Malikova AB. On the determination of spectroscopic constants as functions of intramolecular parameters. J Phys B 1989;22:997–1015.
[50] Nielsen HH. The vibration–rotation energies of molecules. Rev Mod Phys 1951;23:90–136.
[51] Watson JKG. Determination of centrifugal distortion coefficients of asymmetric-top molecules. J Chem Phys 1967;46:1935–49.
[52] Papousek D, Aliev MR. Molecular Vibrational–Rotational Spectra. Amsterdam, Oxford, New York: Elsevier Scientific Publishing Company; 1982.
[53] Antipov AB, Bykov AD, Kapitanov VA, Lopasov VP, Makushkin Y, Tolmachev VI, Ulenikov ON, Zuev VE. Water–vapor absorption spectrum in the 0.59-μm region. J Mol Spectrosc 1981;89:449–59.
[54] Ulenikov ON, Liu AW, Bekhtereva ES, Gromova OV, Hao LY. Hu SM. on the study of high–resolution rovibrational spectrum of H_2S in the region of 7300–7900 cm^{-1} . J Mol Spectrosc 2004;226:57–70.
[55] Zhilinskii BI. Method of Irreducible Tensorial Sets in Molecular Spectroscopy. Moscow: Moscow State University Press; 1981.
[56] Moret-Bailly J, Gautier L, Montagutelli J. Clebsch–Gordan coefficients adapted to cubic symmetry. J Mol Spectrosc 1965;15:355–77.
[57] Rey M, Boudon V, Ch W, Pierre G, Sartakhov B. Orientation of O(3) and $SU(2)\otimes C_i$ representation in cubic point groups (O_h, T_d) for application to molecular spectroscopy. J Mol Spectros 2003;219:313–25.
[58] Loéte M. Développement complet du moment dipolaire des molécules tétraédriques. application aux bandes triplement dégénérées et à la diade ν_2 et ν_4. Can J Phys 1983;61:1242–59.
[59] Saveliev VN, Ulenikov ON. Calculation of vibration–rotation line intensities of polyatomic molecules based on the formalism of irreducible tensorial sets. J Phys B 1987;20:67–83.
[60] Bykov AD, YuS M, Ulenikov ON. On isotope effect in polyatomic molecules. some comments on the method. J Mol Spectrosc 1981;85:462–79.
[61] Bykov AD, YuS M, Ulenikov ON. On the displacements of centers of vibration–rotation bands under isotope substitution in polyatomic molecules. J Mol Spectrosc 1982;93:46–54.